Granular Matter (2018) 20:42
https://doi.org/10.1007/s10035-018-0811-4

ORIGINAL PAPER

Possibility of useful mechanical energy from noise: the solitary wave train problem in the granular chain revisited

Sourish Chakravarty[1,2] · Surajit Sen[3]

Received: 23 July 2017

Abstract
A momentary velocity perturbation at an edge of a granular chain with the grains barely touching one another and held between fixed walls propagates as a solitary wave whereas a long lived perturbation, even if it is noisy, ends up as a solitary wave train. Here, we extend our earlier work but with a force instead of a velocity perturbation. Such a perturbation can propagate an extended compression front into the system. We find that a snapshot of the distribution of grain compressions in the solitary wave train shows *parabolic* as opposed to an *approximate exponential* decay with the leading edge at the front of the traveling pulse and the trailing edge following it. The system's time evolution depends on three independent parameters-the material properties, duration of perturbation and the characteristic amplitude of the perturbation. Hence, the coefficients used to describe the parabolic decay of the grain compressions in the solitary wave train depend on these three parameters. When a random finite duration force perturbation is applied we find that the randomness is smoothed out by the system, which in turn suggests that long granular chains (or equivalent systems, such as circuits) can be potentially useful in converting random noisy signals to organized solitary wave trains and hence to potentially usable energy.

Keywords Granular chains · Nonlinear dynamics · Solitary wave trains

1 Introduction

Wave propagation in granular media is a mature subject [1–4]. The experiments of Nagel and coworkers [5] stimulated an era of strong activity in studies of mechanical energy propagation in granular materials and this burst of activity continues to this day. Much work has been done on ultrasonic propagation in these nonlinear systems [6], on wave propagation in porous, nonlinear systems [7], on using sound bursts to detect buried landmines [8], on seismic wave propagation in soil [9] and more recently on the frequency spectra of propagating sound waves in soil [10–12].

We consider a linear alignment of monodispersed spherical beads of mass m with the beads barely touching each other. When this system is excited at one end by a δ-function perturbation, a solitary wave (SW) is created [13–21]. However, when excited by a finite-duration perturbation at one end, a sequence of solitary waves [a solitary wave train (SWT)] eventually emerges and travels towards the other end [13–15]. In earlier work, we have examined the SWT formation problem when the initial condition is characterized by a bead of mass M_0 moving with a fixed velocity and hitting the edge where $M_0 \leq m$ and $M_0 > m$ [22,23]. Here we consider the case of a force perturbation generated over *finite* time duration to an edge grain. It turns out that the pattern of solitary wave amplitudes in the SWT is sensitive to the nature of the initial perturbation at the same mechanical energy input. The energies carried by the SWs in the SWT arising from extended time force perturbation at one end of the granular chain is therefore different compared to the results discussed in our previous work [22]. To get an intuitive understanding of this difference we observe that an extended time force perturbation ends up generating a spatially extended com-

✉ Sourish Chakravarty
sc267@buffalo.edu

Surajit Sen
sen@buffalo.edu

[1] Department of Mechanical and Aerospace Engineering, The State University of New York at Buffalo, Buffalo, NY 14260-1500, USA

[2] Present Address: The Picower Institute for Learning and Memory , Massachusetts Institute of Technology, Cambridge, MA 02139, USA

[3] Department of Physics, The State University of New York at Buffalo, Buffalo, NY 14260-1500, USA

Published online: 22 June 2018

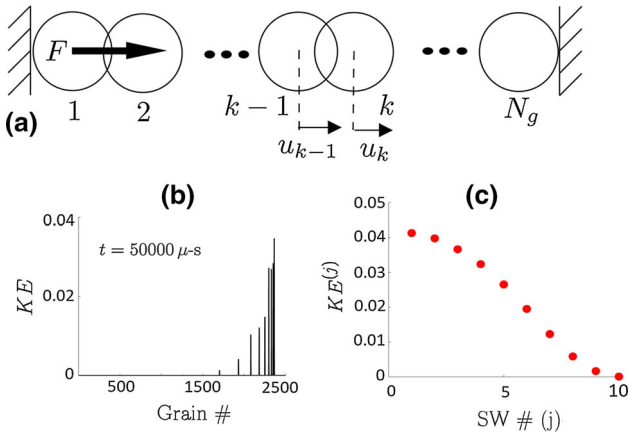

Fig. 1 The subfigure **a** in the top-panel illustrates the model used for short-duration force excitation incident on one end of a granular chain resulting in a SWT. The kinetic energy (KE) state at time instant $t = 50,000\,\mu$s is depicted in the left subfigure **b** of the bottom-panel. In the right subfigure **c** of the bottom panel the KE in the ith SW packet is plotted for the fully formed state SWT. The most energetic SW is labeled as 1, the second most as 2 and so on. Simulation parameters for this particular illustration are: $\theta = 0$, $N_g = 4000$, $R = 9\,$mm, $Y = 110\,$GPa, $\nu = 0.34$, $M = 13.25\,$g, $F_c = 0.7\,$kN, $T_p = 500\,\mu$s and $T_{\text{simu}} = 10{,}000\,\mu s$

pression pulse in the chain. The formation of such a pulse has the profound effect of altering the sequence of grain-grain compressions eventually in the fully formed SWT.

The dynamics of the system is governed by the nonlinear contact interaction force between two adjacent beads. The Hertz potential between the two beads turns out to be, $V \propto r^{5/2}$; where r is the relative compressive deformation between the two beads [24–26]. The index of the power law, 5/2, enters from the circular/elliptical cross-section at the bead–bead interface and will be different if the cross-section is different. A study of the fundamental nonlinear equations indicates that an analogous problem can also be realized in nonlinear electrical circuits [27]. We will restrict to the case of spherical beads in this study.

The purpose of this paper is two-fold: (1) To capture the characteristic parameters of the *fully formed* SWT as a function of system and perturbation parameters. In this fully formed state, the individual SWs in the SWT are clearly distinguishable and its characteristics are approximately[1] invariant over the rest of the simulation time. Our study is based on numerical simulations of the nonlinear dynamical system (Fig. 1a). (2) To analyze the SWT formed from random fluctuations in the applied force and contrast it against the deterministic case. The latter line of inquiry shows that the deterministic model can still be utilized to analyze the conversion of a noisy input signal into an ordered sequence of energy packets. Thus such a model may have potential application in the conversion of random noise to useful mechanical energy. The approach to our study is empirical—we perturb the system and perturbation parameters in the numerical model of this system and then analyze its asymptotic response. This simulation-based approach is useful to build an understanding of the input–output relationship for such a highly nonlinear system whose response is dependent on the nature of perturbation. Even though our approach is empirical, the numerically-developed models proposed here can be used to predict asymptotic SWT response for the system-under-consideration under uniform perturbation force profile.

[1] Computationally calculated values of response of the SWT, even after a long simulation time, will fluctuate over simulation time increments, but a time averaging of the response over an appropriately-chosen time-window can give a reasonable estimate of its fully formed state value.

2 The model system

We consider N_g spherical beads confined between two fixed rigid walls. The chain is excited by a random external compressive force $\boldsymbol{F}(t)$ defined as (1) (random quantities shown in bold notation),

$$\boldsymbol{F}(t) = F_c(1 + \boldsymbol{\epsilon}(t)), \tag{1}$$

and applied at the center of the first (from the left) bead. Here, F_c denotes the average force, $\boldsymbol{\epsilon}(t) \in (-\theta, \theta)$ represents a uniform white noise [28] and θ denotes a positive real number. The duration of perturbation is from time $t = 0$ to $t = T_p$, T_p being the period during which the extended perturbation is imparted, after which the external perturbation is stopped and the system dynamics is allowed to evolve up to the simulation time, $t \equiv T_{\text{simu}} \gg T_p$ (see Fig. 1).

The equations of motion (EOMs) are

$$M\ddot{u}_1 = na(-u_1)^{n-1} - na(u_1 - u_2)^{n-1} + F(t)\,, \tag{2a}$$

$$M\ddot{u}_{N_g} = na(u_{N_g-1} - u_{N_g})^{n-1} - na(u_{N_g})^{n-1}, \tag{2b}$$

$$M\ddot{u}_k = na(u_{k-1} - u_k)^{n-1} - na(u_k - u_{k+1})^{n-1}, \tag{2c}$$

where, u_j ($j \in \{1, 2, \ldots, N_g\}$) denotes the displacement of the center of mass of the j-th bead. The last equation (Eq. 2c) is valid for $k \in \{2, \ldots, N_g - 1\}$. The nonlinear contact mechanics between any pair of identical beads is based on the well known Hertz law such that the relevant constant $a = (4/15)(Y/(1 - \nu^2))\sqrt{R/2}$, which holds for a pair of ellipsoidal surfaces in contact ($n = 5/2$) [22,24]. Here, Y, ν, M and R denote the Young's modulus, Poisson's ratio, mass and radius of each bead, respectively. It is important to note that the force term of type $a(u_k - u_{k+1})^{n-1}$, due to the contact between any two consecutive beads [say, kth and $(k + 1)$th beads], will have a non-zero contribution to the relevant EOM of either only if there occurs a relative compression ($u_k - u_{k+1} > 0$).

Table 1 Data set $\mathcal{S}_a$: $n = 5/2$, $\Delta T_{\text{simu}} = 0.001\mu$s and $\Delta T_{out} = 1\mu$s.

ρ	ν	Y	R	T_p	F_c	N_g	T_{simu}
4.42	0.34	110	10.00	500	1.00	4	5
4.42	0.34	110	15.00	500	1.00	4	5
4.42	0.34	110	11.00	500	1.00	4	5
4.42	0.34	110	12.00	500	1.00	4	5
4.42	0.34	110	13.00	500	1.00	4	5
7.85	0.30	200	10.00	500	1.00	4	5
7.85	0.30	200	11.00	500	1.00	4	5
7.85	0.30	200	12.00	500	1.00	4	5
7.85	0.30	200	14.00	500	1.00	4	5

The units of the tabulated values are: ρ (mg/mm^3), Y (GPa), R (mm), T_p (μs), F_c (kN), N_g ($\times 10^3$), T_{simu} ($\times 10^4\mu$s)

The computer program for evolving the system dynamics (Eqs. 2a, 2c) is coded in fortran and executed within Matlab software environment. The time integration is based on a velocity verlet algorithm. We run several simulations for the deterministic case ($\theta = 0$) by varying F from 10^{-1} to 1.3 kN, T_p from 300 to 600 µs, and R from 8 to 14 mm (across Tables 1, 2, 3). The material properties considered are prescribed by Young's modulus (Y), Poisson's ratio (ν) and density (ρ) triples representing titanium ($Y = 110$ GPa, $\nu = 0.34$, $\rho = 4.42$ mg/mm^3) and steel ($Y = 200$ GPa, $\nu = 0.3$, $\rho = 7.85$ mg/mm^3) as in Table 1. The simulation conditions are such that $N_g \sim 4000$–6000, $T_{\text{simu}} \sim 5 \times 10^4$ µs and fixed time step $\Delta T_{\text{simu}} = 0.001$ µs. The large system size is necessary because we are seeking the evolution of a finite time perturbation into a fully formed SWT. For a typical simulation, the relative error in total mechanical energy content in the system between the instant T_p (after which no external work is done on the system) and any other time instant $t \le T_{\text{simu}}$, is in the order of 10^{-6}. Experimental verification of the work developed here may be possible for systems of beads for which the dissipation, by design and construction, is very small and the acceleration measurements are highly accurate.

To identify the SWT from the dynamical response, we extract the observations over a suitable time window $t \in [T_l, T_{\text{simu}}]$, such that $T_l \gg T_p$, at a time interval $\Delta T_{out} = 1$ µs (appropriately chosen for computational efficiency while not losing out on quality of the data). The time instant T_l is numerically determined such that after this time point and until T_{simu}, the number of distinct SW packets, N_{swt}, does not vary and that any ith SW in the SWT maintains its characteristic width, linear momentum $P^{(i)}$ and mechanical energy $E^{(i)}$. The SWs are numbered as per the decreasing order of their amplitude, where the leading SW with the highest amplitude is labeled as 1, the second highest as 2 and so on. We use time averaged (over $[T_l, T_{\text{simu}}]$) values of the relevant SWTs—thus averaging the error (of small magnitude) introduced due to numerical integration. It should be emphasized here that the SWs form in time as a result of the extended perturbation and then order themselves with the ordering process involving interactions between the SWs [29–32]. The process of creation and self-sorting of the SWs into SWT is a complex phenomenon which is still not well understood for granular chains and remains an open research question.

To develop the algebraic relationships, mentioned above, we find a particular re-parameterization of the EOMs (Eqs. 2a, 2c), using the relative compression $r_{j-1,j}$ ($= u_{j-1} - u_j$), to be helpful. By defining two scaled variables $\widetilde{r}_{j-1,j} \equiv M r_{j-1,j}$ ($j \in \{1, 2, \ldots, N_g + 1\}$) and $\widetilde{a} \equiv a/M^{n-1}$, the revised EOMs are given by,

$$\ddot{\widetilde{r}}_{0,1} = -n\widetilde{a}\,\widetilde{r}_{0,1}^{n-1} + n\widetilde{a}\,\widetilde{r}_{1,2}^{n-1} + F. \tag{3a}$$

$$\ddot{\widetilde{r}}_{N_g,N_g+1} = n\widetilde{a}(\widetilde{r}_{N_g-1,N_g})^{n-1} - n\widetilde{a}(\widetilde{r}_{N_g,N_g+1})^{n-1} \tag{3b}$$

$$\ddot{\widetilde{r}}_{k-1,k} = n\widetilde{a}\,\widetilde{r}_{k-2,k-1}^{n-1} - 2n\widetilde{a}\,\widetilde{r}_{k-1,k}^{n-1} + n\widetilde{a}\,\widetilde{r}_{k,k+1}^{n-1}, \tag{3c}$$

where the first two equations (Eqs. 3a, 3b), respectively, describe the bond dynamics at the contact between each of the two boundary beads and the fixed boundaries, whereas the last equation (Eq. 3c) describes the bond dynamics at every bead-bead contact. Therefore, $\widetilde{r}_{0,1} = M(-u_1)$ and $\widetilde{r}_{N_g,N_g+1} = M(u_{N_g})$. Here, F represents the excitation term (random or deterministic). As discussed earlier for Eqs. (2a–2c), a force term of type $a\widetilde{r}_{j-1,j}$ would have a non-zero contribution in the above equations only if it represents a compression ($\widetilde{r}_{j-1,j} > 0$). The above reparameterization can be interpreted as if we are visualizing the system comprising of discrete masses as made up of only nonlinear springs (active only in compression). This is inspired by the dual transformation in Toda's works [33,34].

By studying the revised EOMs (Eqs. (3a–3c)), keeping in mind Eq. 1, it can be inferred that, for a given n, the properties of the fully formed SW depend on the system parameter, $\widetilde{a}$, and perturbation parameters, F_c and T_p. We have examined various ways of describing the sequence of maximum grain compressions for the fully formed SWT. It turns out, surprisingly, that a simple quadratic model describes the observed behavior better than an exponential model. Using this fit, the maximum relative compression (amplitude) of the ith SW is represented by,

$$r_{\max}^{(i)} = A(i-1)^2 + B, \tag{4}$$

where A and B are constants depending on a, M, F_c and T_p. Note that B equals the amplitude of the leading SW (for $i = 1$) and $A < 0$. In Fig. 2 we contrast this quadratic amplitude attenuation for the short duration force perturbation case with that of an exponential amplitude attenuation in SWT resulting in the same system when subject to velocity perturbation [22,

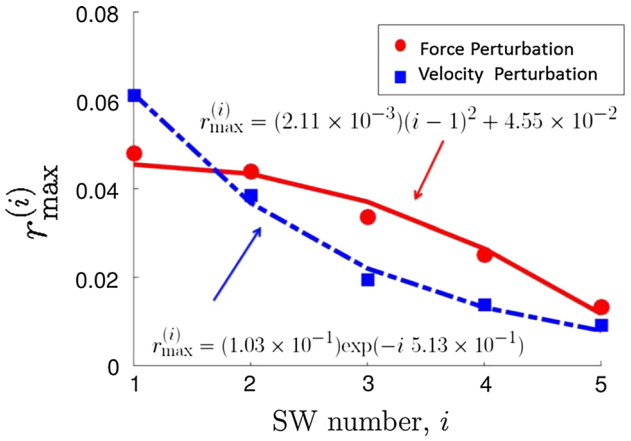

Fig. 2 Plot of SW amplitude ($r^{(i)}_{\max}$) versus SW number (i) at 10000 μs corresponding to the leading 5 SWs (that capture the most of the total mechanical energy) for force and velocity perturbation cases. SWs are numbered in the decreasing order of maximum amplitude. Simulation parameters are: $\rho = 4.6\,\text{mg/mm}^3$, $\nu = 0.36$, $Y = 120\,\text{GPa}$, $R = 12.5\,\text{mm}$, $N_g = 5000$, $T_{\text{simu}} = 60,000\,\mu\text{s}$. For the force perturbation case, $F_c = 1.1\,\text{kN}$ and $T_p = 375\,\mu\text{s}$. For the velocity perturbation case, the velocity of striker-mass (Grain 1 with mass = 5M) is such that its kinetic energy equals the mechanical energy input for the force perturbation case (= 0.3596 J). This ensures that the comparison of the fully formed SWT between the force and the velocity perturbation cases can be performed with same total energy in both

23]. The quadratic amplitude attenuation in Eq. 4 is suggested for the specific case of short duration force perturbation. It may be noted that a similar quadratic form was invoked to describe the SWT structure that emerges for the Korteweg-de Vries equation [4].

The simulations reveal the dependence of the parameters in Eq. 4 on the system and the perturbation parameters. The range of system and perturbation parameters considered in this study, although narrow, is of practical interest. Force perturbation initiated at one end of the granular chain for extended times has the effect of creating an extended compression pulse that starts off near the perturbed end. Such an extended compression pulse was not seen in the velocity perturbation cases we examined earlier [22,23]. The nature of this problem is such that typically the system makes a small number of SWs in the fully formed SWT. Our simulations reveal that for the system sizes we are able to probe, typically there are 5–10 SWs in the SWT that eventually form and end up as separate SWs in the fully formed SWT. We next focus on characterizing the functional forms of the dependences of A and B on a, M, F_c and T_p. Given the strongly nonlinear nature of this problem, it is difficult to intuit these functional forms. Assuming that A and B would likely not have any characteristic scale associated with their dependences on a and F_c, we choose to model them to have algebraic as opposed to exponential dependences on these parameters. We note that increasing the magnitude of T_p may not mean indefinite increase in the size of the first SW in the fully formed SWT. The validity of Hertz law and the time scale of interaction between the grains would likely set the largest SW that would form and the number of trailing SWs in the SWT. This leads us to expect a possible saturation type behavior in how A and B would depend upon T_p. For this reason, at the simplest level, we expect an exponential dependence of A and B on T_p. As we shall see, these assumptions turn out to work for our purposes.

3 Numerical study of the deterministic external perturbation

3.1 Dependence of $r^{(i)}_{\max}$ on system and perturbation parameters

To analyze the functional dependence of A and B (in Eq. 4) on the perturbation and material parameters, the relevant equation is rephrased for convenience as follows,

$$\widetilde{r}^{(i)}_{\max} = \widetilde{A}(i-1)^2 + \widetilde{B}, \text{ where} \tag{5}$$

$$\widetilde{r} = Mr; \quad \widetilde{A} = MA; \quad \widetilde{B} = MB. \tag{6}$$

Note that $\widetilde{B}$ corresponds to the $\widetilde{r}^{(1)}_{\max}$ of the leading SW with the highest amplitude and $\widetilde{A} < 0$ ensures that the function is decreasing with increasing SW index. The term $\widetilde{A}$ governs the rate at which the function will decrease. This means that for a given $\widetilde{B}$ a higher $|\widetilde{A}|$ will correspond to a lower number of SWs with significant energy in the SWT as compared to a lower value of $|\widetilde{A}|$ which would correspond to a higher number SWs in the SWT. The results from the dynamical simulations for n fixed at 5/2 are consistent with the following ansatz,

$$\widetilde{A} = -C_A\,(\widetilde{a})^{\gamma_1}\,(F_c)^{\gamma_2}\left[\exp(\gamma_3 T_p)\right], \tag{7}$$

$$\widetilde{B} = C_B\,(\widetilde{a})^{\beta_1}\,(F_c)^{\beta_2}\left[1-\exp(\beta_3 T_p)\right]. \tag{8}$$

Note that the parameters γ_3 and β_3 must be negative to ensure the saturation behavior of $\widetilde{A}$ and $\widetilde{B}$ with increasing T_p. As we shall see, Eq. 4 reliably captures the quadratic trend shown in Fig. 2. Currently, our understanding of the detailed nature of multibody collisions in the granular chains is limited to the pictures developed in the binary collision approximation [35] and as argued elsewhere [21,36], deeper understanding of the consequences of the non-integrable nature of the problem is needed to develop a theoretical basis for Eqs. (7) and (8).

To evaluate the exponents and multiplication factors, we perform a sensitivity analysis by perturbing each set of parameters $\widetilde{a}$, F_c and T_p one at a time while keeping the other two fixed, and updating the model as each dependence is characterized. The analysis leading up to the exponents and multiplication factors, is performed in three stages.

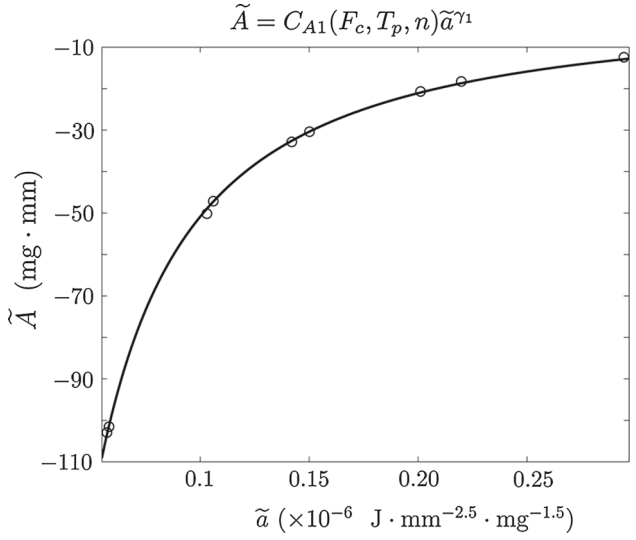

Fig. 3 Dependence of A on a and M characterized by a dependence of $\widetilde{A}$ on $\widetilde{a}$ using data set $\mathcal{S}_a$. Circles and solid line represent simulation data and fitted curve, respectively

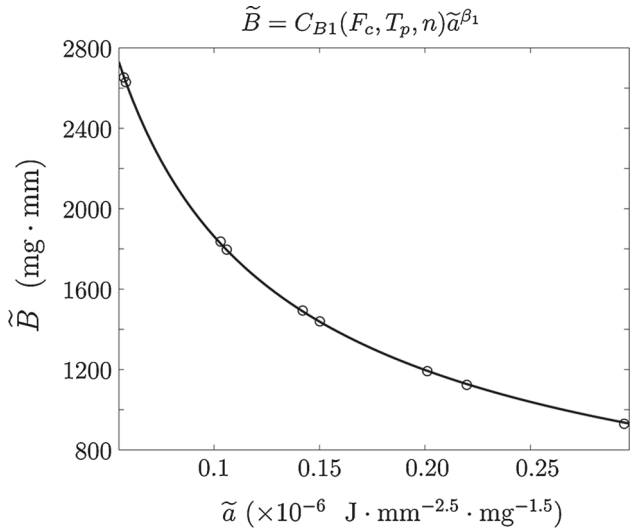

Fig. 4 Dependence of B on a and M characterized by a dependence of $\widetilde{B}$ on $\widetilde{a}$ using data set $\mathcal{S}_a$. Circles and solid line represent simulation data and fitted curve, respectively

In the first stage, using the evaluated values of $\widetilde{A}$ and $\widetilde{B}$ corresponding to input data set $\mathcal{S}_a$ (Table 1) we fit the following trend curve,

$$\widetilde{A} = C_{A1}(F_c, T_p, n)\widetilde{a}^{\gamma_1}, \text{ and} \tag{9}$$

$$\widetilde{B} = C_{B1}(F_c, T_p, n)\widetilde{a}^{\beta_1}, \tag{10}$$

to evaluate γ_1 and β_1, where C_{A1} and C_{B1} are constants conditioned on fixed F_c, T_p and n. The quality of the curve fitting is demonstrated in Figs. 3 and 4.

In the second stage, using the simulation results of $\widetilde{A}$ and $\widetilde{B}$ corresponding to input data set $\mathcal{S}_b$ (Table 2) we fit the following trend curve,

$$-\frac{\widetilde{A}}{\widetilde{a}^{\gamma_1}} = C_{A2}(T_p, n)F_c^{\gamma_2}, \text{ and} \tag{11}$$

$$\frac{\widetilde{B}}{\widetilde{a}^{\beta_1}} = C_{B2}(T_p, n)F_c^{\beta_2}, \tag{12}$$

to evaluate γ_2 and β_2, where C_{A2} and C_{B2} are constants conditioned on fixed T_p and n. The quality of the curve fitting is demonstrated in Figs. 5 and 6.

Table 2 Data set $\mathcal{S}_b$: $n = 5/2$, $\Delta T_{\text{simu}} = 0.001\mu\text{s}$, $\Delta T_{out} = 1\mu\text{s}$

ρ	ν	Y	R	T_p	F_c	N_g	T_{simu}
4.42	0.34	110	8	500	0.10	4	5
4.42	0.34	110	8	500	0.20	4	5
4.42	0.34	110	12	500	3.20	8	6
4.42	0.34	110	12	500	0.50	4	6
4.42	0.34	110	12	500	0.90	4	6
4.42	0.34	110	12	500	1.00	4	6
4.42	0.34	110	12	500	1.50	4	6
4.42	0.34	110	12	500	2.00	4	6
7.85	0.30	200	12	500	0.30	4	6
7.85	0.30	200	12	500	0.60	4	6
7.85	0.30	200	12	500	0.70	4	6
7.85	0.30	200	12	500	0.80	4	6
7.85	0.30	200	12	500	0.90	4	6
7.85	0.30	200	12	500	1.00	4	6
7.85	0.30	200	12	500	1.20	4	6
7.85	0.30	200	12	500	1.30	4	6

The units of the tabulated values are: ρ (mg/mm^3), Y (GPa), R (mm), T_p (μs), F_c (kN), N_g ($\times 10^3$), T_{simu} ($\times 10^4\mu$s)

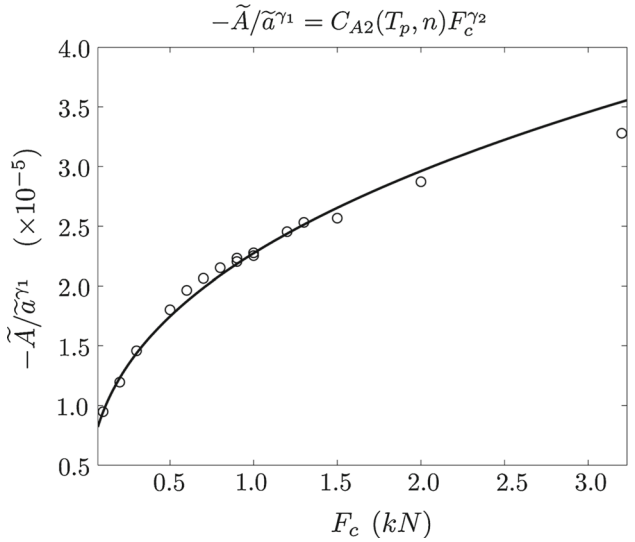

Fig. 5 Dependence of A on F_c using data set $\mathcal{S}_b$. Circles and solid line represent simulation data and fitted curve, respectively

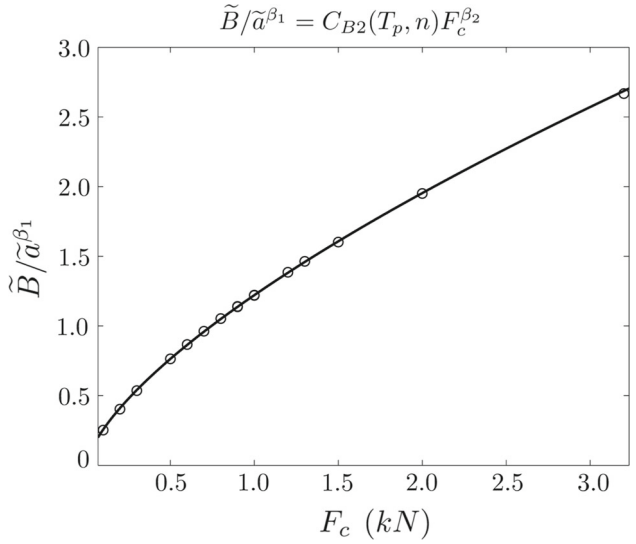

Fig. 6 Dependence of B on F_c using data set $\mathcal{S}_b$. Circles and solid line represent simulation data and fitted curve, respectively

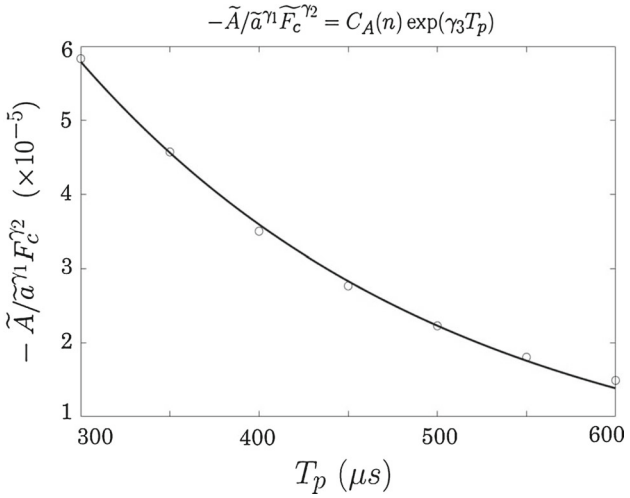

Fig. 7 Dependence of A on T_p using data set $\mathcal{S}_c$. Circles and solid line represent simulation data and fitted curve, respectively

Table 3 Data set $\mathcal{S}_c$: $n = 5/2$, $\Delta T_{\text{simu}} = 0.001\mu$s, $\Delta T_{out} = 1\mu$s

ρ	ν	Y	R	T_p	F_c	N_g	T_{simu}
7.85	0.30	200	8	300	0.25	4	5
7.85	0.30	200	8	350	0.25	4	5
7.85	0.30	200	8	400	0.25	4	5
7.85	0.30	200	8	450	0.25	4	5
7.85	0.30	200	8	500	0.25	4	5
7.85	0.30	200	8	550	0.25	4	5
7.85	0.30	200	8	600	0.25	4	5

The units of the tabulated values are: ρ (mg/mm^3), Y (GPa), R (mm), T_p (μs), F_c (kN), N_g ($\times 10^3$), T_{simu} ($\times 10^4$ μs)

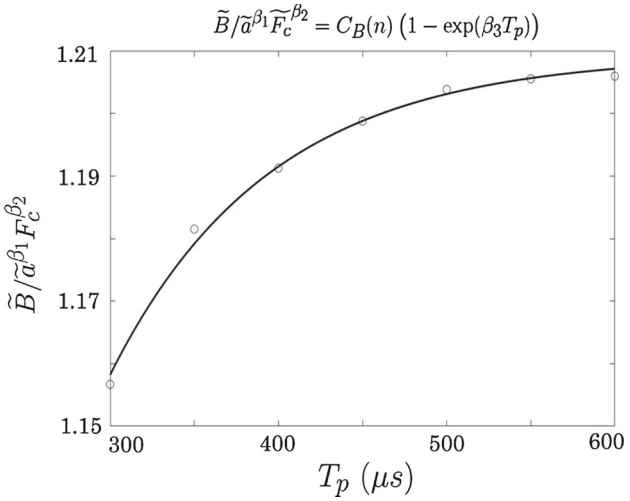

Fig. 8 Analysing the dependence of B on T_p using data set $\mathcal{S}_c$. Circles and solid line represent simulation data and fitted curve, respectively

In the third stage of model parameter estimation, we use the simulation results of $\widetilde{A}$ and $\widetilde{B}$ corresponding to input data set $\mathcal{S}_c$ (Table 3) to fit an algebraic trend curve based on,

$$-\frac{\widetilde{A}}{\widetilde{a}^{\gamma_1}F_c^{\gamma_2}} = C_A(n)\left[\exp(\gamma_3 T_p)\right], \text{ and} \tag{13}$$

$$\frac{\widetilde{B}}{\widetilde{a}^{\beta_1}F_c^{\beta_2}} = C_B(n)\left[1 - \exp(\beta_3 T_p)\right], \tag{14}$$

where C_A and C_B are constants conditioned on fixed n. The quality of the curve fitting is demonstrated in Figs. 7 and 8. The parameters C_A and C_B are determined using all three data sets $\mathcal{S}_a$, $\mathcal{S}_b$ and $\mathcal{S}_c$ and are given in Table 4.

In summary, the numerical data and corresponding curve-fits presented so far indicate that the SWT amplitude attenuation parameters (A and B in Eq. 4) depend on the system and perturbation input parameters (Eqs. 7, 8). Our functional forms here suggest that the formation of the SWT for extended force perturbation is a highly complex problem of distribution of mechanical energy and momentum within a large, strongly nonlinear chain.

3.2 Dependence of $E^{(i)}$ and $P^{(i)}$ on $r_{\max}^{(i)}$, system and perturbation parameters

Once functional dependence of $r_{\max}^{(i)}$ on the system and perturbation parameters is modeled, the next step is to model the mechanical energy and linear momentum content in a solitary wave. It is observed from the numerical observations that the ratios K_P and K_E described as per,

Table 4 Parameters governing the dependence of A and B on a, M, F_c and T_p

Parameter	Value	Data set
γ_1	-1.27	$\mathcal{S}_a$
γ_2	0.381	$\mathcal{S}_b$
γ_3	-4.77×10^{-3}	$\mathcal{S}_c$
β_1	-0.637	$\mathcal{S}_a$
β_2	0.678	$\mathcal{S}_b$
β_3	-1.05×10^{-2}	$\mathcal{S}_c$
Parameter	**Mean**	**SD**	**Data set**
C_A	2.46×10^{-4}	0.007×10^{-3}	$\mathcal{S}_a, \mathcal{S}_b, \mathcal{S}_c$
C_B	1.22	0.009	$\mathcal{S}_a, \mathcal{S}_b, \mathcal{S}_c$

Data sets used for parameter evaluation mentioned. Note that γ_3 and β_3 have units of $(\mu s)^{-1}$, γ_1, γ_2, β_1 and β_2 are non-dimensional numbers and C_A and C_B have units such that $\widetilde{A}$ and $\widetilde{B}$ have units of $mg.mm$ based upon Eqs. 7 and 8, respectively

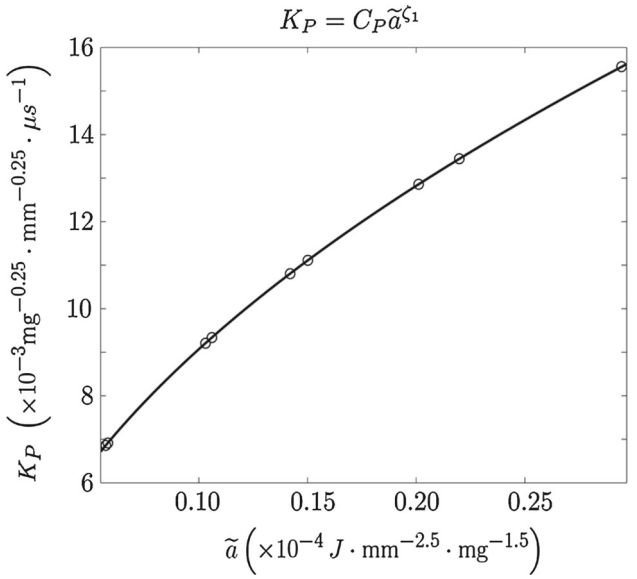

Fig. 9 Dependence of K_P on $\widetilde{a}$ using $\mathcal{S}$. Circles and solid line represent simulation data and fitted curve, respectively

$$K_P = \frac{P^{(i)}}{\left(M r_{\max}^{(i)}\right)^{\frac{5/2}{2}}} = C_P \widetilde{a}^{\zeta_1}, \text{ and} \tag{15}$$

$$K_E = \frac{E^{(i)} M}{\left(M r_{\max}^{(i)}\right)^{5/2}} = C_E \widetilde{a}^{\zeta_2} \tag{16}$$

obey the power-law dependence only on $\widetilde{a}$. For fully formed SWs, these ratios are expected to be independent of F_c and T_p; this has also been numerically confirmed within a desired level of accuracy. Again using input data set $\mathcal{S}_a$ (Table 1) we fit a power-law trend curve to obtain the exponents ζ_1 and ζ_2 and constants C_P and C_E. The quality of the curve fitting is

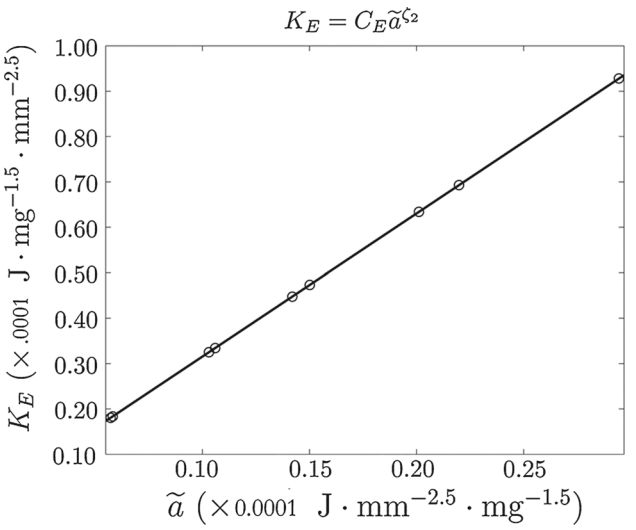

Fig. 10 Dependence of K_E on $\widetilde{a}$ using data set $\mathcal{S}$. Circles and solid line represent simulation data and fitted curve, respectively

Table 5 Parameters determining the dependence of $P^{(i)}$ and $E^{(i)}$ on a, M, F_c and T_p

Parameter	Value	Data set
ζ_1	0.5	$\mathcal{S}_a$
ζ_2	1	$\mathcal{S}_a$
Parameter	**Mean**	**SD**	**Data set**
C_P	2.86	1.61×10^{-4}	$\mathcal{S}_a, \mathcal{S}_b, \mathcal{S}_c$
C_E	3.13	1.39×10^{-3}	$\mathcal{S}_a, \mathcal{S}_b, \mathcal{S}_c$

demonstrated in Figs. 9 and 10 and the resulting parameters are presented in Table 5.

The proposed expressions for $P^{(i)}$ and $E^{(i)}$ can be summarized as,

$$P^{(i)} = C_P \left(M r_{\max}^{(i)}\right)^{\frac{5/2}{2}} \left(\frac{a}{M^{n-1}}\right)^{\zeta_1} \tag{17}$$

$$E^{(i)} = \frac{C_E}{M} \left(M r_{\max}^{(i)}\right)^{5/2} \left(\frac{a}{M^{n-1}}\right)^{\zeta_2}. \tag{18}$$

Note that in the above equations the number $5/2$ is preserved for some terms because it may turn out to be n, but this inference cannot be drawn from the current study which is for fixed $n = 5/2$. On the other hand, the n in the definition of $\widetilde{a}$ term can be preserved as an algebraic term since it comes directly from the re-parameterization of the dynamical equations.

We propose that an approximation for N_{swt} can be the SW number greater than which all the SWs will take non-positive values for $r_{\max}^{(i)}$ according to Eq. 4. By setting left-hand-side to zero in Eq. 4 and solving for this particular SW number, we propose the equation below,

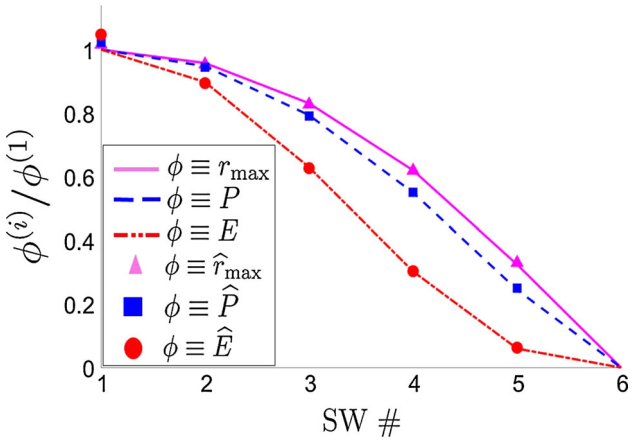

Fig. 11 Normalized SWT response versus SW number. Simulated observations ($\widehat{\phi}$) are compared with corresponding values ϕ from the assumed model. Simulation parameters are: $\rho = 4.6\,\text{mg/mm}^3$, $\nu = 0.36$, $Y = 120\,\text{GPa}$, $R = 12.5\,\text{mm}$, $T_p = 375\,\mu\text{s}$, $F_c = 1.1\,\text{kN}$, $N_g = 5000$, $T_{\text{simu}} = 60{,}000\,\mu\text{s}$

$$N_{\text{swt}} \approx \left\lfloor 1 + \sqrt{(-B/A)} \right\rfloor , \tag{19}$$

to predict the number of SWs in the SWT. Here, for any real number q, $\lfloor q \rfloor$ denotes its greatest integer lower bound. Since this equation is derived from Eq. 4 which models the amplitude trend across multiple SWs in the SWT, this model cannot capture the $N_{\text{swt}} = 1$ case.

It is important to note, and as can be seen later, that typical values of $r_{\max}^{(i)}$, which we use to fit Eq. 4, vary over a decade or so. The SWTs spanning this range capture more than 99.99% of the total energy content in the systems considered here. The energetics for each SW obey the ratio $E_K^{(i)}/E_V^{(i)} = 1.25$, where $E_K^{(i)}$ and $E_V^{(i)}$, respectively, denote the kinetic and potential energies in the i-th SW and $E^{(i)} = E_K^{(i)} + E_V^{(i)}$. These energies are calculated as per,

$$E_K^{(i)} = \sum_{j=N_L^{(i)}}^{N_R^{(i)}} M(\dot{u}_j)^2/2 , \tag{20}$$

$$E_V^{(i)} = \sum_{j=N_L^{(i)}}^{N_R^{(i)}} a(\max\{r_{j-1,j},\, 0\})^{5/2} , \tag{21}$$

where $N_L^{(i)}$ and $N_R^{(i)}$, respectively, denote the labels of the left boundary grain and right boundary grain that support the i-th SW once it is numerically identified from the simulation results. To test the accuracy of the assumed model, the system is simulated with a new set of input parameters (a, R, M, T_p, F_c) which were not used while estimating the model. One such validation study is demonstrated in Fig. 11 and the model, developed so far, is seen to reasonably capture the observed SWT response.

4 The random force perturbation problem

When the external excitation is random with noise about the average force F_c, as seen in the fixed force perturbation problem, once again there develops an extended region of space in the granular chain where the grains end up being compressed simultaneously and eventually a SWT emerges for the granular system under consideration. The system redistributes the perturbed energy input in the same pattern as in the deterministic case. We observe that no new SWs are created in the SWT due to the randomness itself. However, the input fluctuations show up as very small fluctuations in the energy content in each SW in the fully formed SWT as can be seen in Fig. 12. This implies that, just like the deterministic input energy is "quantized" into SWs in the SWT, the fluctuation too gets quantized initially within the SWs in the SWT. Since SWs with more energy move faster than those with less energy, the fully formed SWT ends up being practically identical whether or not there are random fluctuations in the initial force perturbation. This observation needs further mathematical analysis which is outside the scope of the current paper.

The case depicted in Fig. 12 is where the same system as in Fig. 11 is simulated with a noisy excitation by considering $\epsilon(t)$ as a uniform white noise input and maintaining $\theta = 1$ in Eq. 1. The total energy input into the system is 0.3596 J for the deterministic case and 0.3586 J for the random case. In both cases, 0.9995 of the total input energy is contained in the SWT. The results shown in Fig. 12 are for six different time instants after the perturbation is switched off. The panels in Fig. 12 suggest that the SWT eventually formed captures the input energy in the random case well.

Since the error due to the random fluctuation in the fully formed SWT response (say, at $t = 50,000\,\mu\text{s}$) is negligible, one can use Eqs. (7) and (8) to construct the SWT due to the noisy excitation.

5 Useful mechanical energy from noise

The expectation that the mechanical energy in a noisy force perturbation can eventually end up being distributed among a sequence of SWs in a SWT led to this study. As shown above, we see that the properties of the SWT can be characterized quite accurately for relatively simple noisy signals. However, such simple noisy signals also perhaps are expected if one could harvest mechanical energy vibrations in bridges due to continuous pedestrian and/or automobile traffic, along the surface of a ship due to the continuous interfacing with the waves, in busy highways for significant parts of weekdays, or perhaps in many manufacturing plants. One then wonders whether it is possible to use such noisy force fluctuations into harvestable energy. The answer as we can see is, in prin-

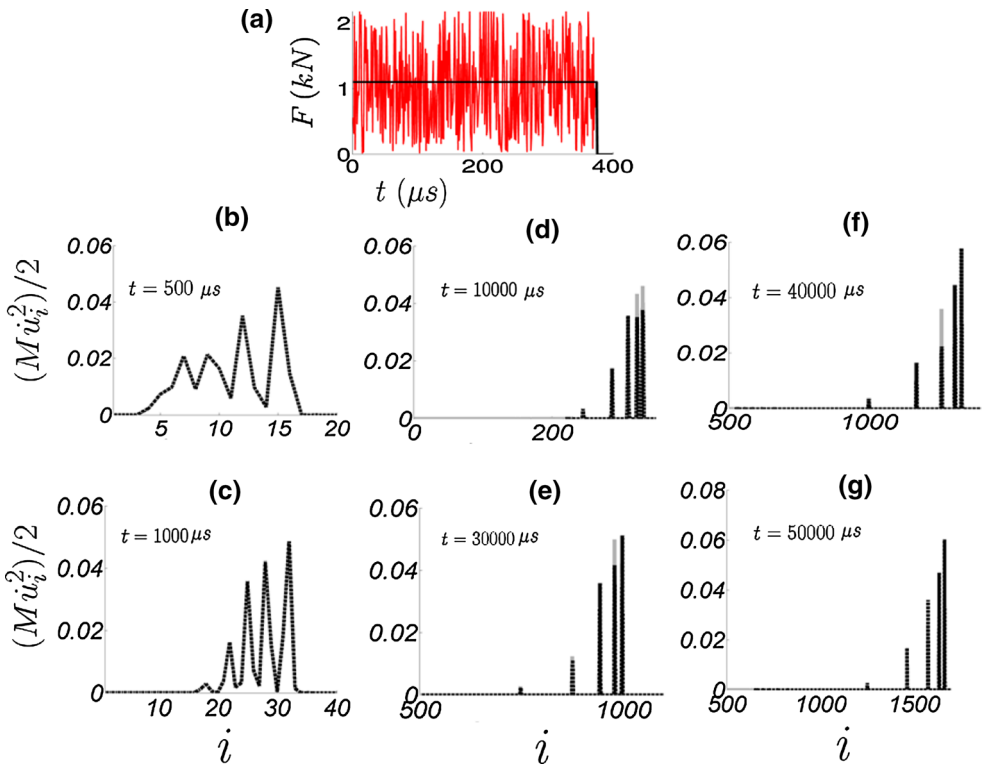

Fig. 12 A single realization of random force versus time is given at the very top subfigure **a** where the black solid line illustrate the average force and the red line depict the fluctuation about the average force. For the random realization the simulation parameters are: $\theta = 1$, $N_g = 5000$, μs, $R = 12.5\,\text{mm}$, $Y = 120\,\text{GPa}$, $\nu = 0.36$, $M = 37.629\,\text{g}$, $F_c = 1.1\,\text{kN}$, $T_p = 375\,\mu\text{s}$. In the other subfigures **b** through **g** the kinetic energy KE (Joule) is plotted versus bead number for 6 time points. In subfigures **b** through **g** the response due to the random force (black solid lines) are overlaid on the response due to an applied constant force equaling the average of the random case (gray solid lines)

ciple, yes. However, granular systems are macroscopic in nature and hence inherently dissipative. Can one make very long nanogranular systems perhaps to see if dissipation can be reduced? [37,38]. The answer to this question is unknown. However, even nanoscale grains have some dissipation. One possible way out of this dissipation issue is to use an integrated circuit to replace the granular chain. The integrated circuit serves the role of converting the input signal by partitioning it into SWs that make up a SWT where A and B are constructed using various circuit elements to realize Eqs. (7) and (8) [27]. Such integrated circuits require power to function in an effectively non-dissipative manner. Hence, using integrated circuits to convert noisy input forces to useful electrical energy in this case would only be worthwhile when the power needed to run the circuit is low enough and hence the cost inexpensive enough compared to the harvested power. Whether this is possible is a topic of exploration in the future.

It is natural to wonder what might be the limits of noise that can be converted to useful energy or a SWT. Since SWT formation needs sufficient system size and hence time, one must have a sufficiently large system to handle a highly noisy input force perturbation. Further, the amplitude of the noise cannot be so high that the Hertz law which holds for elastic compression of the grains becomes invalid. Both of these problems are no longer important however if one is using an integrated circuit to effectively represent the input signal by a SWT using Eqs. (7) and (8) for a large enough system.

A recent work [39] has proposed analytical expressions characterizing the dependence of peak force and momentum content within a SWT on the perturbation and system parameters for a chosen input force profile. Even though this work [39] considers a different perturbation, the analytical approach proposed in this work suggests possible ways of exploring the problem considered here.

6 Conclusion

Here we have developed expressions to describe the properties of the fully formed SWT for any system described by Eqs. (2a), (2b), and (2c). The properties depend upon the geometric and material parameters (effectively one parameter) of the system and the external perturbation parameters (amplitude of the perturbing force and the time across which the force acts).

We show that the developed expressions can also be used to characterize the SWT when the input external force perturbation has an additive white noise over a constant value. Hence, when a random force is incident at one end of a long granular chain, the system can convert this noisy input into a well-organized SWT with minimal error. In reality a long granular chain with near zero dissipation would be a handy system to use to convert a noisy input force into a SWT that can then be transformed to useful electrical energy. Given our expressions in Eqs. 4 through 8, it may be possible to design a circuit to convert the energy imparted via an extended time input force perturbation into a SWT with each SW in the train carrying the amount of momentum and energy given by Eqs. 17 and 18, where $r_{\max}^{(i)}$ is given by Eq. 4 and A and B are given by Eqs. 7 and 8, respectively [27].

Acknowledgements We are grateful to the US Army Research Office for partial support of the work reported here. We would like to thank Robert W. Newcomb and Gary F. Dargush for their interest in the work. SC thanks Abhishek Venketeswaran and Kundan Goswami for useful discussions.

Compliance with ethical standards

Conflict of interest The authors declare that they have no conflict of interest.

References

1. Biot, M.A.: Mechanics of deformation and acoustic propagation in porous media. J. Appl. Phys. **33**(4), 1254–1264 (1962)
2. Biot, M.A.: Mechanics of deformation and acoustic propagation in porous dissipative media. J. Appl. Phys. **34**(9), 1482–1498 (1962)
3. Hardin, B.O., Richart, F.E.: Elastic wave velocities in granular media. J. Soil. Mech. Found. Div. **89**, Proc. Paper 3407 (1963)
4. Karpman, V.I.: Nonlinear Waves in Dispersive Media. Pergamon Press Ltd., Oxford (1974)
5. Liu, C.-H., Nagel, S.R.: Sound in a granular material: disorder and nonlinearity. Phys. Rev. B **48**(21), 15646 (1993)
6. Jia, X., Caroli, C., Velicky, B.: Ultrasound propagation in externally stressed granular media. Phys. Rev. Lett. **82**(9), 1863–1869 (1999)
7. Makse, H.A., Gland, N., Johnson, D.L., Schwartz, L.: Granular packings: nonlinear elasticity, sound propagation, and collective relaxation dynamics. Phys. Rev. E **70**(6), 061302 (2004)
8. Sen, S., Krishna Mohan, T.R., Visco, D.R., Swaminathan, S., Sokolow, A., Avalos, E., Nakagawa, M.: Using mechanical energy as a probe for the detection and imaging of shallow buried inclusions in dry granular beds. Int. J. Mod. Phys. B **19**(18), 2951–2973 (2005)
9. O'Donovan, J., Ibraim, E., O'Sullivan, C., Hamlin, S., Muir Wood, D., Marketos, G.: Micromechanics of seismic wave propagation in granular materials. Granul. Matter **18**(03), 1–18 (2016)
10. Gilcrist, L.E., Baker, G.S., Sen, S.: Preferred frequencies for three unconsolidated earth materials. Appl. Phys. Lett. **91**(25), 254103 (2007)
11. Shrivastava, R.K., Luding, S.: Wave propagation of spectral energy content in a granular chain. EPJ Web Conf. EDP Sci. **140**, 02023 (2017)
12. Shrivastava, R.K., Luding, S.: Effect of disorder on bulk sound wave speed: a multiscale spectral analysis. Nonlinear Process Geophys. **24**(3), 435 (2017)
13. Nesterenko, V.F.: Propagation of nonlinear compression pulses in granular media. J. Appl. Mech. Tech. Phys. **24**(5), 733–743 (1983)
14. Lazaridi, A., Nesterenko, V.F.: Observation of a new type of solitary waves in a one-dimensional granular medium. J. Appl. Mech. Tech. Phys. **26**(3), 405 (1985)
15. Nesterenko, V.F.: Dynamics of Heterogenous Materials. Springer, New York (2001)
16. Sinkovits, R.S., Sen, S.: Nonlinear dynamics in granular columns. Phys. Rev. Lett. **74**(14), 2686–2689 (1995)
17. Sen, S., Sinkovits, R.S.: Sound propagation in impure granular columns. Phys. Rev. E **54**(6), 6857–6865 (1996)
18. Coste, C., Falcon, E., Fauve, S.: Solitary waves in a chain of beads under Hertz contact. Phys. Rev. E **56**(5), 6104–6117 (1997)
19. Chatterjee, A.: Asymptotic solution for solitary waves in a chain of elastic spheres. Phys. Rev. E **59**, 5912–5919 (1999)
20. Mouraille, O., Mulder, W.A., Luding, S.: Sound wave acceleration in granular materials. J. Stat. Mech. Theory Exp. **07**, 07023 (2006)
21. Sen, S., Hong, J., Bang, J., Avalos, E., Doney, R.: Solitary waves in the granular chain. Phys. Rep. **462**(2), 21 (2008)
22. Sokolow, A., Bittle, E.G., Sen, S.: Formation of solitary wave trains in granular alignments. Europhys. Lett. **77**, 24002 (2007)
23. Job, S., Melo, F., Sokolow, A., Sen, S.: Solitary wave trains in granular chains: experiments, theory and simulations. Granul. Matter **10**, 13–20 (2007)
24. Hertz, H.: Über den kontakt elastischer körper. J. reine angew. Math. **92**, 156–171 (1881)
25. Sun, D., Daraio, C., Sen, S.: Nonlinear repulsive force between two solids with axial symmetry. Phys. Rev. E **83**, 066605 (2011)
26. Goldsmith, W.: Impact—The Theory and Physical Behavior of Colliding Solids. Edwards Arnold, London (1960)
27. Sellami, L., Newcomb, R.W., Sen, S.: Simulink modeling for circuit representation of granular chains. Mod. Phys. Lett. B **27**, 1350093 (2013)
28. Bolotin, V.V.: Random Vibrations of Elastic Systems—Mechanics of Elastic Stability 8. Martinus Nijhoff, The Hague (1984)
29. Manciu, M., Sen, S., Hurd, A.J.: Crossing of identical solitary waves in a chain of elastic beads. Phys. Rev. E **63**, 016614 (2000)
30. Manciu, F.S., Sen, S.: Secondary solitary wave formation in systems with generalized Hertz interactions. Phys. Rev. E **66**, 016616 (2002)
31. Job, S., Melo, S., Sokolow, A., Sen, S.: How Hertzian solitary waves interact with boundaries in a 1D granular medium. Phys. Rev. Lett. **94**, 178002 (2005)
32. Santibanez, F., Munoz, R., Caussarieu, A., Job, S., Melo, F.: Experimental evidence of solitary wave interaction in Hertzian chains. Phys. Rev. E **84**(2), 026604 (2011)
33. Toda, M.: Vibration of a chain with nonlinear interaction. J. Phys. Soc. Jpn. **22**, 431 (1967)
34. Toda, M.: Waves in nonlinear lattice. Prog. Theor. Phys. Suppl. **45**, 174 (1970)
35. Rosas, A., Lindenberg, K.: Pulse velocity in a granular chain. Phys. Rev. E **69**, 037601 (2004)
36. Przedborski, M., Sen, S., Harroun, T.A.: Fluctuations in Hertz chains at equilibrium. Phys. Rev. E **95**, 032903 (2017)
37. Takato, Y., Sen, S., Lechman, J.: Strong plastic deformation and softening of fast colliding nanoparticles. Phys. Rev. E **89**, 033308 (2014)
38. Takato, Y., Benson, M.E., Sen, S.: Granular chains with soft boundaries: slowing the transition to quasi-equilibrium. Phys. Rev. E **91**, 042207 (2015)
39. Hasan, M.A., Nemat-Nasser, S.: Universal relations for solitary waves in granular crystals under shocks with finite rise and decay times. Phys. Rev. E **93**, 042905 (2016)